Thermal Analysis of a Lorentz Force Accelerator with an Open Lithium Heat Pipe *

G. Emsellem†, A. D. Kodys ‡, E.Y. Choueiri §
Electric Propulsion and Plasma Dynamics Laboratory (EPPDyL)
MAE Dept.
Princeton University, Princeton NJ 08544.

IEPC-99-166¶

Abstract

A three dimensional thermal analysis of a Lorentz force accelerator featuring an open heat pipe as a propellant feeding system is made in order to correct heat transfer problems that became apparent during attempts to operate the device. Specifically, the temperature profile along the multi-channel cathode of the thruster, which is also the open end of the heat pipe, was such that the cathode tip stayed at a temperature well below the vapor point of lithium thus causing lithium vapor to condense in the cathode. An empirically inspired solution was first implemented and consisted in outfitting the cathode assembly with a series of closed heat pipes that are heated form outside the truster. However, the heat pipes failed to operate properly due to nearby thermal sinks that caused them to choke. The numerical thermal model showed what these sinks are and was instrumental in the implementation of a scheme that resulted in the successful operation of the thruster.

*This work is supported through an SBIR contract from NASA-JPL through Thermacore Inc. and by a grant from NASA-JPL's Advanced Propulsion Group.

†Graduate Student, Ecole Normale Superieure de Lyon, AIAA Student member

‡Graduate Student, AIAA Student member.

§Chief Investigator at EPPDyL. Assistant Professor, Applied Physics Group. Senior Member AIAA.

¶Presented at the 26^{nd} International Electric Propulsion Conference, Kitakyushu, JAPAN, October 17-21, 1999.

1 Introduction

1.1 The Li-LFA and the MPDT

The lithium Lorentz force accelerator (Li-LFA) is a variant of the steady-state magnetoplasmadynamic thruster (MPDT) that uses lithium as propellant and a multi-channel cathode. The MPDT has demonstrated its capability of providing a specific impulse (I_{sp}) in the range of 1500 to 8000 s with thrust efficiencies exceeding 40%[1]. High efficiency (above 30%) is typically reached only at high power levels (above 100 kW) (see Ref. [2] for instance) and consequently the steady-state version of the MPDT is regarded as a high-power propulsion option. It has the unique capability, among all developed electric thrusters, of processing very high power levels (MW-level) in a simple, small and robust device producing thrust densities as high as 10^5 N/m^2. These features have rendered the steady-state MPDT particularly attractive for deep-space energetic (high Δv) missions requiring high thrust levels such as manned and cargo spacecraft to Mars and the outer planets[3] as well as for nearer-term orbit raising missions[4, 5]. The present unavailability of high power in space and the cathode erosion rates of the steady-state MPDT (which can be as high as 0.2 μg/C), have until recently impeded the evolution of steady-state MPDTs towards flight applications.

A version of the steady-state MPDT, called the lithium Lorentz force accelerator (Li-LFA), that uses a multi-channel hollow cathode and lithium for propellant promises to solve the cathode erosion problem while significantly raising the thrust efficiency at moderately high power levels[6]. Recently, a thrust efficiency of 43% at an I_{sp} of 3460 s was measured in Moscow[7] for a low-erosion Li-LFA operating at 130 kW. The thrust-to-power ratio of these devices is typically about 25 N/MW. The extension of the lifetime of such thrusters to above 1000 hours has been recently shown to be within reach with the demonstration of 500 hours of practically erosion-free operation of a 50%-efficient Li-LFA at 0.5 MW [8]. Since no other single electric thruster has yet demonstrated the capability of processing that much power (500 kW), producing that much thrust (12.5 N), and operating that long (500 hours) without significant erosion, the Li-LFA is at the forefront of propulsion options for nuclear-powered deep space human exploration and heavy cargo missions to the outer planets.

Due to these reasons the Li-LFA is presently the focus of much interest at NASA[9, 10].

1.2 Background

A collaboration between Thermacore Inc. and Princeton University's EPPDyL, resulted in the development of a 100-kW class Li-LFA that uses a novel lithium feeding system. Since the lithium feeding subsystem is generally the most complex part of the Li-LFA system, the primary focus was on the development of a feeding system that does not use any moving mechanical parts or valves. Heat pipe technology was adapted in the form of a heat pipe whose one (closed) end is the propellant storage reservoir and the other (open) end is the multi-channel cathode of the thruster through which lithium vapor is fed to the discharge. The open heat pipe lithium Lorentz force accelerator is referred to as OHP-Li-LFA.

The design of the thruster and the calibration methodology for the open-heat pipe feed system have already been described in detail in ref. [11]. While the system is quite simple mechanically, the thermal design and mass flow calibration proved to be quite challenging problems that required much empirical, numerical and testing efforts at both Thermacore and EPPDyL.

The focus of this paper is on the detailed thermal analysis that was conducted subsequent to the first attempt to fire the thruster when it became clear that the original thermal design of the system did not allow for the lithium vapor to reach the cathode tip without condensing. The results of this thermal analysis were instrumental in devising and implementing a scheme that led to the successful operation of the thruster.

It is relevant to emphasize that the efforts detailed here did not have for a goal the operation and study of the thruster at power levels where the efficiency is good (i.e. near and above 100 kW) but rather the demonstration of the feasibility of the open heat pipe lithium feeding concept.

2 Description of the OHP-Li-LFA

As already mentioned the design of the thruster as well as the concepts behind the open heat pipe lithium feeding system and the associated calibration methods were the subjects of a previous paper[11]. A brief description is given her for the sake of completeness.

2.1 General Description

A cross-sectional schematic of the design is shown in Fig. (1). The drawing shows the dimensions of the component and traces the flow of lithium through the heat pipe that acts as the propellant reservoir. A 3-D schematic of the LFA is shown in Fig. (2).

The open-ended heat pipe provides a novel alternative to the complex propellant feeding systems previously used with lithium-fed thrusters. Aside from simplicity, reliability is enhanced by the fact that there are no valves or moving parts. The closed end of the heat pipe acts as a reservoir containing a liquid lithium pool, and a wick. The main part of the pipe is embedded in a furnace (1200° C) which vaporizes the lithium off the wick. The lithium vapor then travels to the open end which is also the cathode of the LFA supplying the propellant for the plasma thruster. Capillary forces draw up additional lithium from the reservoir to replace the vaporized lithium. The actively heated cathode is a hybrid hollow-multi-channel cathode consisting of 48 longitudinal channels embedded in a porous tungsten insert. (This insert was eventually replaced by a multi-rod assembly in the second version of the thruster used for the present study.) The vaporizer design of the reservoir was deemed superior to a pool boiler for our particular application. Compared with more conventional fluids, alkali metals have high nucleation superheats, high bubble growth rates, long waiting times between bubble nucleations, and high natural convection rates. These conditions can cause problems with unstable boiling and with incipient boiling superheats. In unstable boiling, the heat trans-

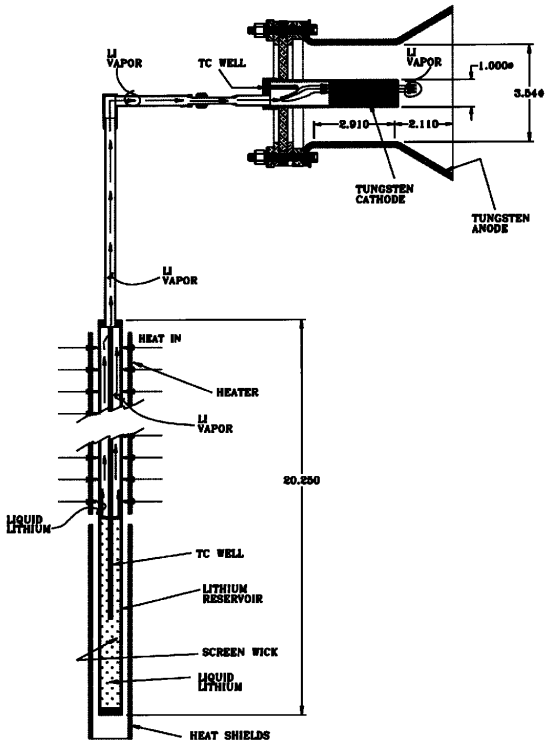

Figure 1: Cross-sectional schematic of the accelerator showing dimensions (in inches) and the flow of lithium vapor.

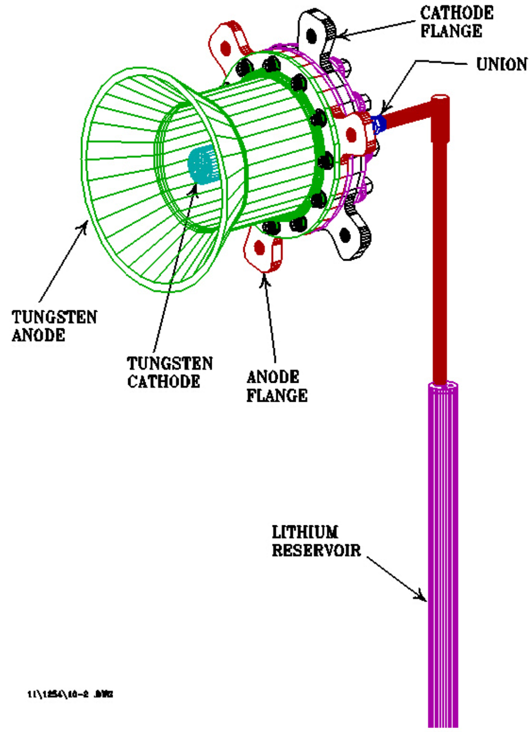

Figure 2: 3-D schematic of the accelerator.

fer mechanism oscillates between nucleate boiling and liquid natural convection, sometimes resulting in violent shaking of the system. The vaporizer design eliminates potential pool boiling problems.

Some of the more important design parameters, dimensions, materials and subsystems of the OHP-Li-LFA are listed in Table 1 of ref. [11].

3 Statement of the Thermal Problem

Steady-state lithium vapor flow through the cathode in the first attempt to fire the thruster was hampered because the lithium was not hot enough, and emerged from the cathode as a liquid. Furthermore, there is a possibility that lithium pooled in the cathode before traveling downstream, which would have been detrimental to the requirements of steady flow.

It is desirable that the cathode should at all points be above the boiling point of lithium. Previous attempts to raise cathode temperature have been of limited effectiveness due to the fact that the cathode heater was placed at one end of the cathode, and the temperature fell rapidly from there to the tip.

This fall in temperature can be characterized by the effective heat conduction of the cathode

$$\frac{\sigma \epsilon C}{kA},$$

where σ is the Stefan-Boltzmann constant, ϵ the emissivity, k the thermal conductivity, A the cross-sectional area and C the external circumference. It can be seen that, for a hollow cylinder, the ratio above is much larger than for a solid cylinder of the same external radius. This means that those parts of the cathode where the porous tungsten insert is not present have a steeper temperature drop than those where the insert is present.

It thus became apparent that a better method is required to insure that a higher temperature profile can be maintained along the cathode so that its tip can be kept above the boiling point of lithium.

This realization led to the design and manufacture

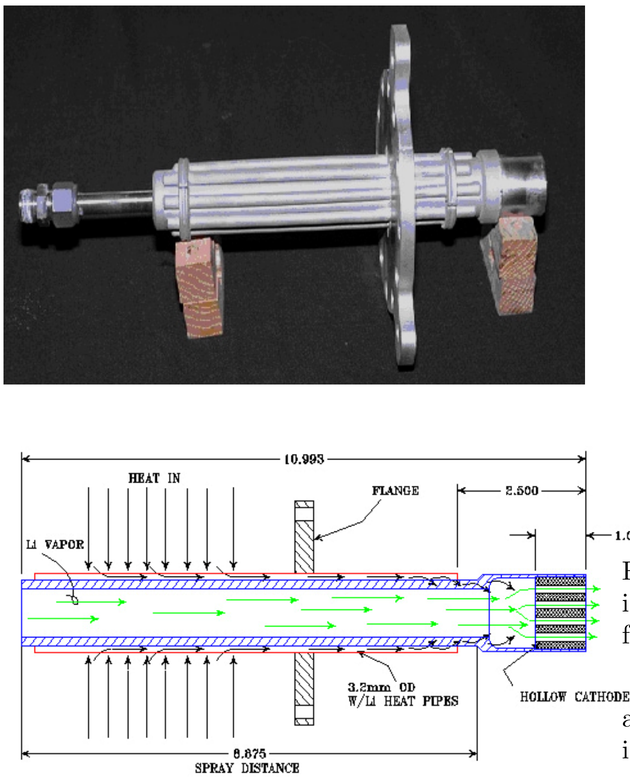

Figure 3: Improved Li-LFA tungsten cathode assembly (top: photo; bottom: schematic) showing eight closed heat pipes along the cathode for better control of cathode temperature.

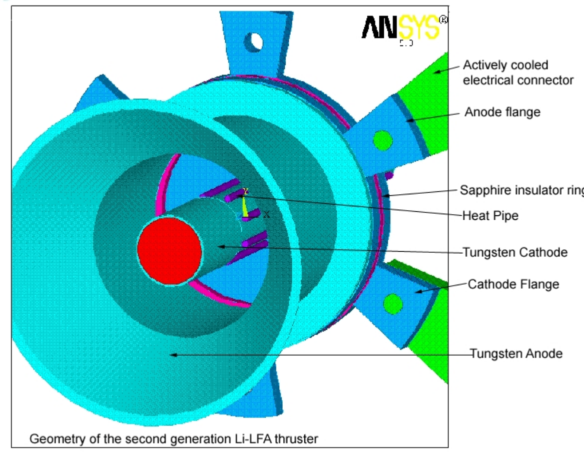

Figure 4: 3-D model of the thruster used for numerical thermal simulations. The colors denote the different materials.

of a new cathode assembly by Thermacore. The main change was that the new assembly now featured eight axial closed lithium heat pipes azimuthally symmetric along the outside jacket of the cathode as shown in as shown in Fig. (3). The heat pipes conduct heat from a dedicated heater (custom-manufactured by Advanced Ceramics Corporation) applied on the part of the cathode extending behind the backplate flange.

Unfortunately this did not lead to an operational thruster as subsequent experiments showed the cathode tip temperature to be well below the 800°C mark needed to avoid lithium liquid to flow out of the cathode tip.

This required a concentrated thermal modeling effort at EPPDyL to explain the thermal behavior of the system, solve the problem and implement a solution that can be implemented without further major alterations to the design. This effort and the resulting insight are described in the following sections.

4 3-D Thermal Modelling

4.1 Description of Model

A finite element model of the new thruster was created using ANSYS to compute the temperature profile during the pre-firing heating phase. The purpose of this effort was to simulate the thermal behavior of the thruster and to provide insight on how to modify the design in order to increase the temperature of the cathode tip thus making the thruster operational. The model could also serve to provide more insight into refining the mass flow calibration.

The asymmetric geometry of the heat load and the thruster required the construction of a full tridimensional model as shown in Fig. (4). Despite the apparent axisymmetry of the body of the thruster, the positioning of the actively cooled power lead (one connected to the anode the other to the cathode flange) required a 3-D non-symmetric model. This asymmetry radically changed the temperature profiles in the thruster and has a direct impact on the temperature of the cathode tip as shown by the numerical results as well as by the experimental measurements.

The complexity of the design suggested using a“top-down” approach. Boolean operations between geometric primitives were used to obtain the right shape for each part of the thruster and then generating the finite elements by meshing these primitives. The tungsten anode, its molybdenum flange, the insulating sapphire ring, the molybdenum cathode flange, the actively cooled power leads, the tungsten cathode and the cathode tip insert of tungsten rods have all been modeled by assembling cylinders and cones of different geometry to reproduce as closely as possible the shape of the real thruster parts. Long and narrow cylinders whose thermal conductivity at each point depends on the temperature are used to represent the heat pipes.

The creation of the mesh was done using the roughest setting (corresponding to the largest mesh able to fit to the geometry) to limit the number of elements and nodes. Extensive testing has shown that the results obtained with a rough mesh are precise enough and hardly modified with a finer mesh. All the elements are tetragonal and carry ten nodes (four nodes on the summits plus six nodes in the middle of the edges). All parts were covered by surface radiating elements to simulate the heat losses to the vacuum tank walls. The behavior of each part has been tested individually and then again at each step of assembling the whole model. The final model consists of 127,000 elements each represented by ten nodes.

The thermal loads consist of clamped temperatures of 1720°C on the part of the cathode assembly located under the cathode back heater, and of 25°C on the extreme border of the actively cooled power leads. All the radiative elements radiate toward a hypothetical wall infinitely far and at a room temperature of 25°C (that is the so-called space node). The mutual irradiation or shielding effect is not taken into account. An important consequence of this model is its inability to reflect the thermal gradient inside the cathode flange because this gradient is due to lost radiation coming from the cathode back heater and falling on the back of the flange.

5 Simulation Results and Comparison to Experiments

The temperature of various control points in the thruster was determined by a series of temperature measurements, under the operating conditions of the pre-heating phase and used to refine and validate the model. These measurements were performed using thermocouples placed in various spots and often performed twice with different thermocouples to check on the dependability of the results.

Despite the fact that the model neglects heating due to the surfaces irradiating heat toward each other, the first numerical results produced were hotter than the real thruster. A reason for this surprising behavior lies in the way parts are thermally coupled together in the numerical model. This becomes a problem when the parameters of the mesh of two parts are very different. In fact attempting to thermally link automatically two parts whose mesh parameter (size of the elements) are quite different (as a rule of the thumb : the ratio of one to the other being higher than 5) will lead to a high "apparent" thermal conductivity. This results from the way the software imposes the same temperature on all the nodes contained in a sphere centered on each node of the largest mesh as illustrated in Fig. (5) and explained in the caption of that figure. Thus the length of the effective conductive path seems reduced. This numerical limitation can be avoided by carefully modifying the mesh at the surface interface and by checking the linked created and removing the extra links manually.

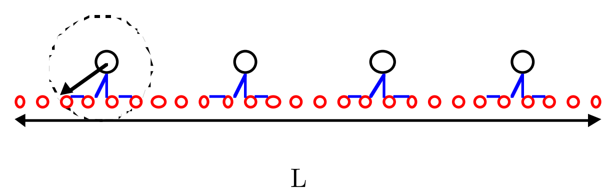

Figure 5: Schematic representation of the method used by the software to link two thermally different parts. The same temperature is applied at all the nodes within a radius r. This reduce the length over which the thermal conduction law is applied. Here the real length is $L = 25a$ (a being the parameter of the smaller mesh) but the conduction law is applied only along $L' = 13a$, so $L' \simeq L/2$ for $A/a = 6.5$ where A is the parameter of the smaller mesh. This would results in an "apparent" doubling of the conductivity.

All initial attempts to reproduce the experimental results using a realistic model of the thermal conductivity of the heat pipes failed. So a simplified curve was generated in which each heat pipe switches between two conductivity states: a low conductivity state (tungsten conductivity) for temperatures below the threshold and a high conductivity state (100 times higher) above this threshold. The threshold became the free parameter of the study. This threshold was initially set at 700°C and raised progressively during the simulation to approach the experimental results. The results were always self-consistent but gave temperatures higher than the measured values by about 200°C. When the threshold was fixed to 1050°C the model reproduced the experimental results at all measurement locations with good accuracy.

The final simulation results are displayed in the table of Fig. (1) along with the measurements and an evaluation of the degree of agreement between the two. The good agreement cleared the way for further use of the model to interpret the experiments and guide further design efforts.

As can be seen in Fig. (6), the model revealed an abrupt transition across the location of the cathode flange from the highly conductive state to the poorly conductive state. The heat pipe are choked there as all the power is transmitted through the cathode flange to the water cooling the power lead. In this situation, the heat pipes behave just like tungsten pipes along the cathode. The results are summarized in Table 1 and the Figures (6) to (8) below. The simulated temperature of the cathode backplate (inside surface of the cathode flange) was found to closely resemble the experimentally observed glow pattern on that surface. The simulation clearly and quantitatively illustrated the problem of low cathode tip temperature.

6 Interpretation of the Problem and Implementation of a Solution

The above simulation results showed that the heat pipes are "choked" at the junction with the cathode flange and consequently stop working as heat pipes[1]. The electrical copper leads provide a heat sink for the cathode flange which is also in contact, through the insulator ring, with the anode whose surface area is large. The anode radiates a large fraction of the power even at low temperature (1kW at 500°). Finally the thruster backplate (inside part of the cathode flange) being quite hot (between 600° and 725°) radiates a substantial fraction of the input power straight forward to the outside of the thruster.

This clarification of the problem coupled with a series of experiments using molybdenum radiation shields lead to the implementation of a final solution of the problem which consisted of installing a series of molybdenum radiation shields in three critical places:

1. Disc foils upstream inside the thruster to shield the backplate radiation,

2. Four layers of molybdenum foils wrapped around the outside of the anode assembly to shield heat loss by radiation from the large anode surface,

3. A retractable molybdenum screen plate that is positioned in front the thruster at the anode exit to trap the radiation loss. This screen is removed by a motor after reaching the desired temperature immediately before firing the thruster.

These fixes, illustrated in Fig. (9), proved critical as they finally allowed the cathode tip temperature to be well above the vapor point of lithium leading to a vapor flow through the cathode multi-channels and consequently led to the successful firing of the thruster

7 Firing of the Final Configuration

The thruster was fired successfully five times at approximately the same nominal power of about 6 kW (a current of about 330 A and a voltage of 18 V). EPPDyL's new high-power thrust stand, developed under NASA-JPL support was used to measure a thrust level of about 24 mN within an error bar of 43.5%. This large error was due to signal noise problems that were subsequently solved. The theoretical thrust prediction based on the Maecker law is 25.74 mN for that current level. The thrust-to-power ratio is therefore

[1] Other possible explanations for the failure of the heat pipes can be discounted based on the following arguments related to the potential heat pipe limits. The frozen startup limit cannot be reached since, even at their coldest spot, the temperature of the heat pipes is higher than the lithium melting point (180°C). The vapor continuity limit is relevant when the evaporator temperature is below 800°C which is not the case since it was 1720°C in the experiments. The viscous limit can only hinder the efficiency of a heat pipe but not prevent it from working, and it is only a transient effect. The capillary limit is not applicable as well since at an evaporator temperature of 1720°C, the power limit would be 300 W per heat pipe which was not the case. For the same reason the sonic limit which at this temperature is larger than 50 kW can also be discounted. There is no entrainment limit for liquid metal heat pipes. The heaters are far from having the power required to boil the lithium. Finally, the effective thermal conductivity of the condenser section is very large because of its large area compared to the size of the heat pipe (1/4 of the heat pipe surface) therefore it cannot be a limiting factor for the power that the heat pipe can carry.

Thermocouple Location	Numerical	Experimental	Disagreement
Under Cathode Heater	fixed at 1720°C	1720°C	0%
Center of Cathode Tip	430°C	470°C	4.5%
Cathode Root at Flange	730°C	725°C	0.7%
Backplate/Insulator Ring	580°C	610°C	5.1%
Anode Lip	280°C	305°C	8.5%

Table 1: Results of 3-D numerical simulation and experimental measurements showing good agreement.

about 4 N/MW which is low as typical of the inefficient operation of self-field LFAs at this relatively low power level of 6 kW.

Due to an operator error, the thermocouple data acquisition software was not properly set during the firing phase of the experiments. Luckily, temperature data in the pre-firing (heating) and post-firing (cooling) phases were recorded and these were used to extrapolate the values needed to estimate the mass flow rate during the experiment. Keeping in mind the unquantifiable accuracy of this extrapolation, a mass flow rate of about 1 mg/s of lithium was estimated which leads to a thrust efficiency not exceeding 5%. This is, again, not surprising for operation at such a low power level. The critical ionization current[12] at these conditions is about 330 A corresponding to an electromagnetic acceleration scaling parameter[12] of $\xi \simeq 1$.

During the last run of the firing series, a spurious current attachment appeared at the back of the thruster and led to the termination of the experiment. Subsequent inspection revealed that this arc attachment was due to a lithium vapor leak at the electron-beam welded junction between the cathode tube and the pipe leading to the tantalum Swagelock.

8 Present and Future Plans

EPPDyL's research on Li-LFAs is continuing under NASA-JPL support and a new thruster system consisting of a Li-LFA head developed by the Moscow Aviation Institute (MAI) and a *mechanical* piston-driven lithium feeding system developed by EPPDyL and NASA-JPL is presently being tested. This new thruster has the advantage of having a *liquid* mass feeding system operating at the relatively low temperature of 200°C. (The boiling of lithium does not occur until the liquid reaches the cathode). This avoids a host of high temperature problems related to the use of dedicated heaters and the use of refractory materials and expensive tantalum Swagelock junctions. Moreover, it is simpler to calibrate than the OHP-Li-LFA described in this paper. It is however more complex *mechanically.*

REFERENCES

[1] V. M. Nerheim, A. J. Kelly. TR 32-1196, NASA-JPL, 1968.

[2] V. A. Petrosov, et. al. IEPC 95-104.

[3] R. H. Frisbee, N. J. Hoffman. AIAA 96-3173.

[4] J. E. Polk, R. H. Frisbee, V. B. Tikhonov, S. Semenkhin, V. Kim et. al. AIP Proc.387,**3**, pp1505-1513.

[5] E. Y. Choueiri et. al. *Jour. S. & R.*, 30(6):749-754, 1993.

[6] J. E. Polk, T. J. Pivirotto. AIAA 91-3572.

[7] V. Kim, V Tikhonov, S. Semenikhin. TR NASW-4851, RIAME, MAI, Moscow, Russia, 1997.

[8] V. P. Ageyev, V. G. Ostrovsky. IEPC 93-117.

[9] R. H. Frisbee. AIAA 99-2164.

[10] J. W. Dunning, J. M. Sankovic. AIAA 99-2161

[11] E. Y. Choueiri, V. Chiravalle et. al. . AIAA 96-2737.

[12] E. Y. Choueiri. *Jour. Prop. & Pow.*, 14(5):744-753, 1998.

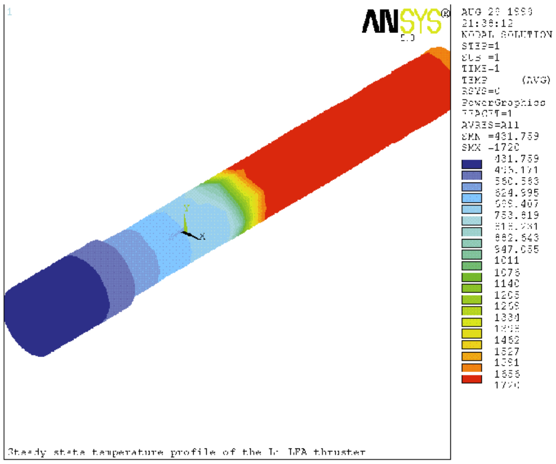

Figure 6: Computed cathode temperature. Note the abrupt temperature drop across the short area where the flange is mounted, and the cold cathode tip.

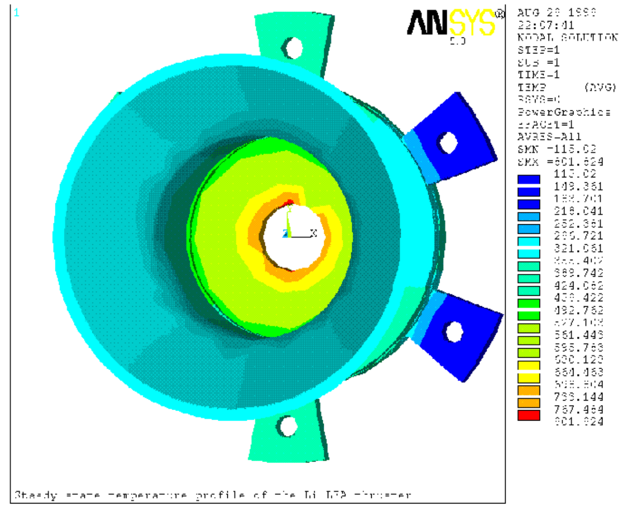

Figure 8: 3-D view of simulation results. The temperature of the cathode backplate (inside surface of the cathode flange) closely resembles the experimentally observed glow pattern.

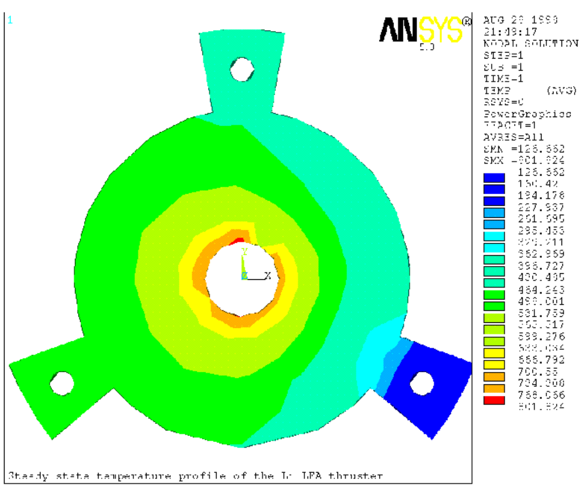

Figure 7: Simulation of cathode flange temperature. Note the strong asymmetry induced by the connection of the actively cooled power leads.

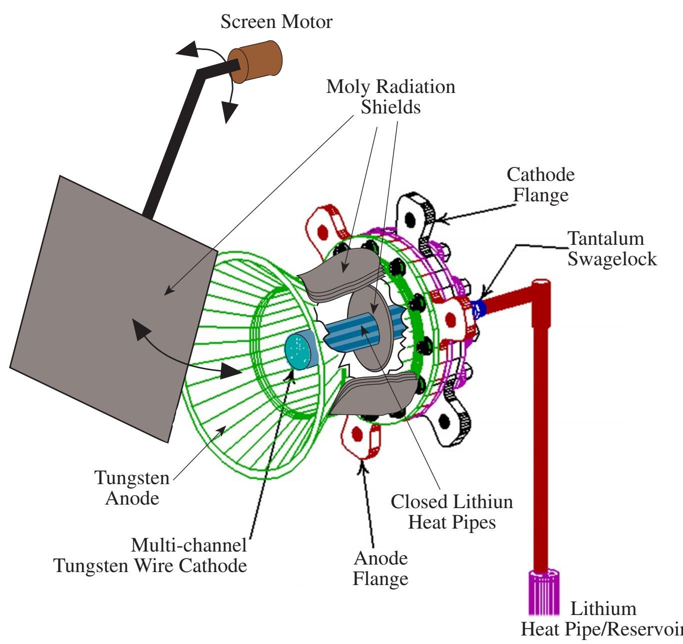

Figure 9: Schematic of the final configuration of the OHP-Li-LFA showing the various molybdenum heat shields that were required to bring the cathode temperature above the vapor point of lithium before firing the thruster.